Jurnal Teknologi

Full Paper

NON-DESTRUCTIVE ANALYSIS OF WHITE A4 OFFICE PAPERS USING ATR-FTIR SPECTROSCOPY AND CHEMOMETRIC PROCEDURES FOR FORENSIC APPLICATION

Wan Nur Syuhaila Mat Desa, Tay Eue Kam, Dzulkiflee Ismail*

Forensic Science Programme, School of Health Sciences, Universiti Sains Malaysia, Health Campus, 16150 Kubang Kerian, Kelantan, Malaysia

Article history
Received
30 April 2025
Received in revised form
23 June 2025
Accepted
13 August 2025
Published Online
30 April 2026

*Corresponding author
dzulkiflee@usm.my

Graphical abstract

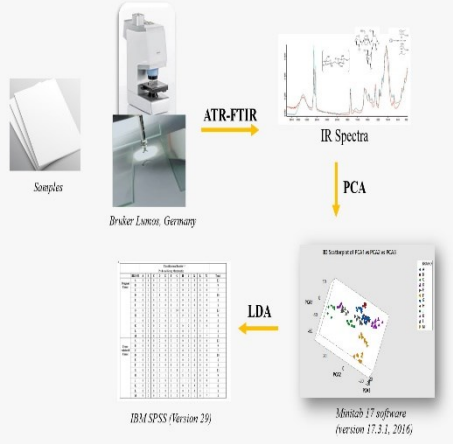

Abstract

In forensic document examination, the physical and chemical properties of paper are important indicators for assessing the authenticity and origin of questioned documents. Preserving the integrity of paper samples is crucial to ensure reliable forensic analysis. Therefore, non-destructive analytical techniques are preferred. This study explores the application of Attenuated Total Reflectance-Fourier Transform Infrared (ATR-FTIR) spectroscopy as a non-destructive method for analyzing commercially available white A4 office papers in Malaysia. ATR-FTIR allows the acquisition of molecular spectral data without damaging the sample, making it suitable for forensic casework. To enhance discrimination and classification performances, chemometrics techniques were employed, integrating Principal Component Analysis (PCA) and Linear Discriminant Analysis (LDA). PCA was used to reduce data dimensionality and identify key spectral patterns, while LDA optimized classification by distinguishing between paper samples based on their spectral characteristics. This approach accounted for 99.96% of the total variance within the first three principal components (PCs) and achieved a cross-validation accuracy of 74.8% using Linear Discriminant Analysis (LDA). These results signify that ATR-FTIR spectroscopy, combined with chemometrics, offers a reliable, rapid, and non-destructive tool for discriminating white A4 office papers. The proposed method has strong potential to enhance forensic document examination by providing an objective and robust approach for document paper analysis.

Keywords: Forensic science, forensic document examiner, questioned documents, infrared spectroscopy, office paper, chemometrics

Abstrak

Dalam bidang pemeriksaan dokumen forensik, sifat fizikal dan kimia kertas merupakan penunjuk penting dalam menilai ketulenan serta menentukan asal usul dokumen yang dipersoalkan. Pemeliharaan integriti sampel kertas adalah sangat penting bagi memastikan analisis forensik yang sah dan boleh dipercayai. Justeru, teknik analisis yang tidak merosakkan amat digalakkan. Kajian ini meneroka aplikasi spektroskopi Attenuated Total Reflectance-Fourier Transform Infrared (ATR-FTIR) sebagai kaedah tidak merosakkan untuk menganalisis kertas pejabat A4 putih yang yang boleh didapati secara komersial di Malaysia. Kaedah ATR-FTIR membolehkan pemerolehan data spektrum molekul tanpa menyebabkan kerosakan kepada sampel, sekali gus menjadikannya sesuai untuk aplikasi kes forensik. Bagi meningkatkan ketepatan

dalam diskriminasi dan pengelasan, pendekatan kimometrik telah digunakan dengan menggabungkan Analisis Komponen Utama (PCA) dan Analisis Diskriminan Linear (LDA). PCA digunakan untuk mengurangkan dimensi data serta mengenal pasti corak spektrum utama, manakala LDA pula berperanan dalam mengoptimumkan pengelasan dengan membezakan sampel kertas berdasarkan ciri-ciri spektrumnya. Pendekatan ini berjaya menjelaskan sebanyak 99.96% daripada jumlah varians melalui tiga komponen utama pertama (PC) dan mencapai ketepatan pengesahan silang sebanyak 74.8% menggunakan LDA. Dapatan ini menunjukkan bahawa gabungan spektroskopi ATR-FTIR dan pendekatan kimometrik merupakan satu kaedah analisis yang boleh dipercayai, pantas dan tidak merosakkan untuk tujuan diskriminasi kertas pejabat A4 putih. Kaedah yang dicadangkan ini berpotensi besar untuk memperkukuh amalan pemeriksaan dokumen forensik melalui pendekatan yang objektif dan teguh dalam analisis melibatkan kertas dokumen.

Kata kunci: Sains forensik, pemeriksa dokumen forensik, dokumen-dokumen yang dipersoakan, spektroskopi inframerah, kertas pejabat, kemometrik

1.0 INTRODUCTION

In the field of forensic science, document paper stands as an integral element in cases involving questioned document examinations. There are frequent situations where it becomes imperative to determine the authenticity of a contested document and verify if it was indeed created during the alleged timeframe. In such instances, aside from analyzing elements like signature authentication, the layout and formatting of the printed text, and the tools employed to prepare the document such as printers or pens, it is also crucial to examine the paper consistency throughout the document. Forensic science adopts a multi-disciplinary approach analysis [1] to establish and furnish additional evidence for the ongoing case. Paper itself serves as another potential piece of evidence. Within a collection of documents presented as evidence, it is important to cross reference the paper used across the entire bundle. Identifying the actual origin or specific characteristics of the paper can serve as additional evidence that may help pinpoint the document's creator.

The paper manufacturing process begins with the preparation of pulp, which is derived from natural sources such as wood, rags, or grasses. This raw material is processed to extract fibers, which are then mixed with water to form a slurry. To enhance paper's properties such as durability and printability, additives like polyvinyl acetate (PVA) and starch are introduced into the pulp mixture [2]. The next step involves forming the paper itself. The pulp slurry is spread onto a large wire screen to create a thin layer. This layer is then pressed to remove excess water and compact the fibers closer together, which helps in forming a strong paper sheet. After pressing, the paper is dried, typically through heated rollers or blowers that evaporate any remaining moisture. To improve the surface properties of the paper, such as its whiteness and texture, coatings are applied. Common substances used in coating include kaolin clay, calcium carbonate ($CaCO_3$), calcium sulfate ($CaSO_4$), and titanium dioxide (TiO_2) [3,4]. These materials fill in the gaps between the fibers, resulting in a smoother and more uniform surface which is ideal for printing and writing.

Different instrumental analysis techniques in the analysis of paper have been deployed. Non-destructive testing is employed to preserve the integrity of the paper sample during analysis. The choice between destructive and non-destructive testing depends on the specific goals of the analysis, the importance of preserving the sample and the objective and type of information required. The destructive analysis methods include X-Ray Diffraction (X-RD) [4], Field-Emission Scanning Electron Microscopy (FE-SEM) [5].Energy-Dispersive X-ray Spectroscopy (EDS) [5], Energy Dispersive X-ray Fluorescence (ED-XRF) [6-10], X-ray Photoelectron Spectroscopy (XPS) [5], Inductive Coupled Plasma Mass Spectrometry (ICP-MS) [6,11,12] and Isotope Ratio Mass Spectrometry (IRMS) [6,13-15]. These approaches analyse the elemental composition in paper such as Mg, Ca, Al, Na, Mn, Fe, Ti, and Sr [5,8,10,12,16-19].

In recent years, there has been a notable shift towards prioritizing non-destructive techniques for assessing the organic and non-organic composition of paper, particularly with the objective of classifying and identifying document paper. Technological advances have spurred the development of various non-destructive analysis methods for paper analysis, such as Raman spectroscopy [20-22], Ultraviolet-Visible UV-VIS [22-26], and Attenuated Total Reflectance Fourier Transform Infrared (ATR-FTIR) spectroscopy [3,20,25,27-35]. These methods allow for detailed organic lignin structure, a fiber binding glue [25] in cellulose fiber and inorganic composition from the coating additives and fillers such as starch, calcium carbonate, casein, crystalline structure of kaolin, talc, titanium dioxide [2] can be analyzed without damaging the documents.

The ATR-FTIR spectroscopy, a non-destructive analysis instrument was used to sample the papers

from different brands in the selected mid-IR region, which ranged between 4000 cm^{-1} to 600 cm^{-1}. The mid-IR region was selected as it is able to provide the absorbance band of the molecular fingerprint of the papers. Within the mid-IR spectrum, specific four regions were identified. They were single bond region (4000 cm^{-1} to 600 cm^{-1}), double bond region (2500 cm^{-1} to 2000 cm^{-1}), triple bond region (2000 cm^{-1} to 1500 cm^{-1}), and the fingerprint region at (1500 cm^{-1} to 600 cm^{-1}) [36]. Several distinct fingerprint regions of paper have been identified in the literature. Pavithra et.al. [25], specifically reported the fingerprint region between 1450 cm^{-1} and 900 cm^{-1}, while other researchers have highlighted regions spanning 1550 cm^{-1} to 750 cm^{-1} [4,34] and 1200 cm^{-1} to 900 cm^{-1} [33].

Chemometrics procedures comprises three primary techniques namely: unsupervised methods, supervised methods, and regression methods [37]. Unsupervised methods, such as Hierarchical cluster analysis (HCA) and Principal component Analysis (PCA), identify patterns without predefined labels, making them useful for exploratory data analysis but unsuitable for classification or regression tasks [37]. PCA, a widely applied multivariate technique, reduces dimensionality by transforming variables into principle components (PCs), which can be visualized using score, loading, or scree plots [38].

Supervised pattern recognition methods utilize labeled data to classify or predict unknown samples, making them essential for individualization, discrimination, and impurity detection [39]. Common supervised methods include k-Nearest Neighbor (kNN), Linear Discriminant Analysis (LDA), Soft Independent Modelling of Class Analogy (SIMCA), Support Vector Machines (SVM), Decision Tree and Random Forest (RF), and Artificial Neural Networks (ANN) [37]. Discriminant Analysis (DA), a key supervised method, enhances class separation by defining discriminant axes (canonical variates) that maximize intergroup differences, while minimizing intragroup variability [38]. LDA is frequently applied after PCA to classify objects into predefined classes while retaining essential dataset information [37,39].

PCA-LDA has been widely employed in chemometric and forensic studies. Kher et. al. [40] used PCA-LDA for spectral analysis of six different types of paper samples, achieving classification accuracies of 95.3% (4000 cm^{-1} – 650 cm^{-1}), 90.6% (2000 cm^{-1} – 650 cm^{-1}), and 53.1% (4000 cm^{-1} – 2000 cm^{-1}). Similarly, Kumar et. al. [41] applied PCA to A4 paper samples, validating results using Pearson Correlation, Kaiser-Meyer-Olkin (KMO) tests, and Bartlett's test, achieving discrimination power (DP) of 99.64%.

PCA-LDA has also been successfully used in forensic applications, such as classifying Raman spectra of inkjet printer ink [42] and discriminating black gel ink [43]. These findings highlight the efficacy of PCA-LDA as a powerful chemometric tool for pattern recognition, classification, and forensic science.

The primary objective of this study was to assess the feasibility of employing non-destructive analytical techniques of Attenuated Total Reflectance-Fourier Transform Infrared (ATR-FTIR) spectroscopy, in combination with chemometric procedures, for the differentiation and classification of white A4 office paper samples according to their brands or manufacturers for forensic document examinations purposes. White A4 papers were selected because they are widely used in the preparation of both official documents (e.g., contracts, wills, and sales agreements) and non-official documents, making them frequently encountered in forensic cases involving document fraud.

2.0 METHODOLOGY

2.1 Sample Collection

This study primarily focused on 70gsm white A4 office papers. A total of twelve reams, each containing 500 sheets of paper, were procured from bookstores, retail outlets and online stores in Malaysia. These 12 reams represented a diverse range of 12 different brands. While some of the brands were commonly known in Malaysia market, other brands, especially those purchased online, were less common. It is noteworthy to mention that, at the time of this study, Malaysia does not have its own office paper manufacturing facility. Consequently, all the office paper procured in this study was either imported or repackaged locally. The paper samples used in this study are shown in Table 1.

Table 1 List of paper samples used in this study

No	Code	Origin	Manufacturer	Brand
1	A	Indonesia	April	Artica
2	B	China	UPM, China	YES UPM
3	C	Indonesia	PT Pinto Deli Pulp and Paper Mills	Copy Paper
4	D	Unknown	Unknown	Top Com Multi-purpose paper
5	E	China	Unknown	Emerald
6	F	China	Fuji Xerox	Fuji Xerox
7	G	Thailand	Double A (1991) Public Co. Ltd	Smartist
8	H	Unknown	Distribution by Rainbow Paper Supplies Sdn Bhd	IK Yelllow Copy Paper
9	J	India	JK Paper Mills & Central Pulp Mills, Gujarat	JK Max
10	K	Indonesia	PT Indah Kiat Pulp & Paper, Perawang Mill	IK Copy Paper
11	L	China	Unknown	Lyreco White Paper
12	M	Indonesia	Unknown – packed in Malaysia	One-Z Copier Paper

Seven sheets of paper samples were randomly selected from different layers within each ream of paper. These selected samples were visually compared both macroscopically and microscopically prior to the ATR-FTIR spectroscopy

2.2 IR Spectra Acquisition

In this study, the IR spectral of the paper samples were acquired using the LUMOS (Bruker, Germany) IR spectrometer equipped with germanium ATR sampling interface. All analyses were conducted at room temperature and ambient humidity conditions. Spectra were obtained within the range between 4000 cm^{-1} to 600 cm^{-1}, employing a scan rate of 64 scans per second, and an illumination intensity of 7%, with measurement collected in absorbance mode.

2.3 Data Acquisition

This study also explored into examining the variation and homogeneity of the composition within the paper. These analyses encompassed several aspects of within a single sheet and between pages from the same ream of paper.

Within each ream, four pieces of paper were sampled from different locations in the ream. In each sheet of these sample sheets, seven specific locations were tested and within each location seven repetitive spectra were collected. This approach resulted in a total of 49 replicates for each paper and a collection of 196 spectral from each ream of paper.

2.4 Data Pre-processing (DP)

In the initial stage, repeatability and reproducibility studies were conducted to ensure consistent measurements were acquired. During ATR-FTIR spectra acquisition, baseline correction was applied to overcome undesirable effects caused by noise, scattering, or radiation. The primary objective of data processing (DP) was to optimize the IR spectra, ensuring it was in optimal condition for improved performance for subsequent analysis.

In addition to the untreated raw data, two scatter-correction pre-processing techniques were applied: namely standard normal variate (SNV) and normalization to total sum [44]. The performance of SNV and normalization was compared and assessed. Assessing both normalized and preprocessed data allows evaluation of the impact of these pre-processing techniques on the chemometrics analysis outcomes.

2.5 Principal Component Analysis (PCA)

A total of 2352 infrared (IR) spectra were collected from the 12 different paper brands and were analyzed using Minitab 17 software (version 17.3.1, 2016). Principal Component Analysis (PCA) was used to explore the data and identify latent patterns. The three-dimensional (3D) score plot from the PCA results made it easier to see how the samples grouped whereby spectra with similar characteristics are positioned close together, while those from different brands were positioned farther apart, indicating separation.

For this analysis, specific wavenumber ranges were selected to focus on areas of the spectrum that contain useful information. These ranges included both the fingerprint region and other key frequency areas. Four distinct wavenumber intervals were used: 3600 cm^{-1} to 2701 cm^{-1} (Region I), 1800 cm^{-1} to 1600 cm^{-1} (Region II), 1499 cm^{-1} to 1300 cm^{-1} (Region III), and 1201 cm^{-1} to 751 cm^{-1} (Region IV). These ranges were chosen because they capture important chemical signals that help differentiate between the brands.

2.6 Linear Discriminant Analysis (LDA)

Linear Discriminant Analysis (LDA) was used to assist in classifying the paper samples based on the patterns found through PCA. LDA works by finding the best way to separate different groups and highlight the differences between them. In this study, the LDA was conducted using IBM SPSS (Version 29), and the cross-validation method was applied to assess how well the classification model performed and how reliable the results were. This approach helped confirm whether the paper samples could consistently be sorted into their respective brand groups.

3.0 RESULTS AND DISCUSSION

3.1 Microscopic Assessments

The visual examination of the paper samples under the microscope revealed general surface features and textural characteristics, including fiber distribution and surface evenness. While these observations provided an initial overview of the paper morphology, no distinct or consistent differences can be recorded in terms of color, luminosity, fluorescent behavior, or fiber arrangement across the 12 different paper brands. The microscopic images, as shown in Figure 1, demonstrate that the fibers and overall appearance of the paper surfaces are visually similar, making it difficult to rely on these features for effective discrimination between brands.

In the context of forensic document analysis, this limitation is crucial. Microscopic analysis, although quick and non-destructive, may not provide the level of discrimination needed when the objective is to link a document to a particular paper brand or manufacturer. This lack of distinct visual variation can potentially lead to inconclusive results when microscopic features are the only method used for assessment of papers.

Therefore, these findings highlight the need for more sensitive analytical techniques in forensic paper analysis. Methods such as ATR-FTIR spectroscopy, paired with chemometric analysis, offer a more

detailed chemical fingerprint of the paper, allowing for greater accuracy in differentiating samples. This step is crucial in forensic examinations, where the ability to distinguish between paper brands can contribute significantly to the authentication of questioned documents and the establishment of evidence.

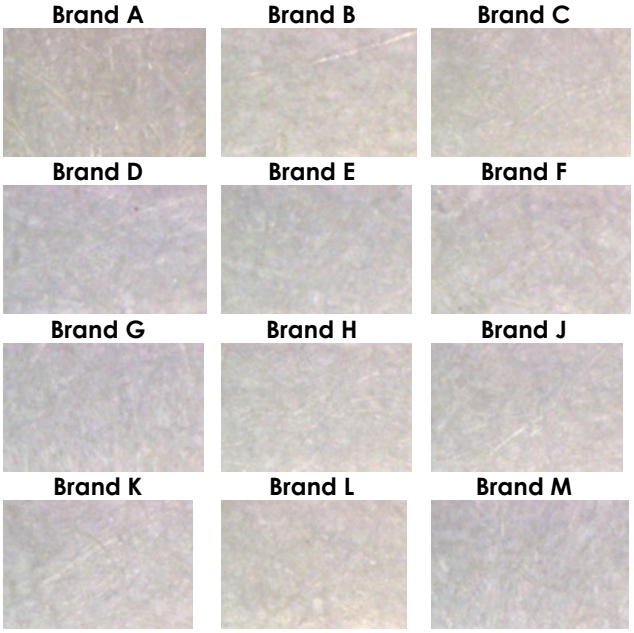

Figure 1 Microscopic images of the paper samples used in the study

3.2 Repeatability and Reproducibility Studies

The repeatability and reproducibility studies demonstrated the robustness of the measurements made in this study. The instrument repeatability recorded low %RSD values (3.14%–4.34%), indicating consistent performance. Within-sheet reproducibility also recorded low variability (%RSD 3.41%–4.39%), confirming that measurements were stable across different areas of the same sheet. Between-sheet reproducibility showed slightly higher %RSD values (up to 5.84%), reflecting natural manufacturing variations but within acceptable limits. Overall, these findings signify that the method is reliable, stable, and capable of producing consistent results, which is essential in forensic analysis of papers to ensure accurate paper classification can be achieved.

The reproducibility analysis result indicates the RSD variations between and among the paper is less than 6%. This explains the spread of composition in the paper around the mean is small, meaning the measurements are consistent and reliable. This level of consistency in the data shows that the variability between the samples is at an acceptable level for further analysis.

3.3 Data Pre-processing Techniques

The evaluation of the three data pre-processing techniques namely untreated (raw data), normalization, and standard normal variate (SNV) revealed marked differences in their impact on variance retention in PCA analysis. As shown in Table 2, normalization provides the highest combined variance for PC1 and PC2 at 84.45%, slightly outperforming the raw dataset (84.02%), indicating improved data consistency and balance without losing too much of useful information. Although the untreated data shows comparable results, normalization ensures better distribution of variance between PC1 and PC2. In contrast, the SNV method resulted in a lower combined variance (79.38%), suggesting a loss of useful information. Despite its good performance in PC1, the reduced PC2 variance highlighted a limitation of SNV for this dataset. Overall, normalization emerged as the most effective pre-processing method approaches for the IR spectra acquired from the paper samples.

Table 2 Comparison results on pre-processing techniques

	Raw	Normalized	SNV
PC1	51.69	49.27	51.03
PC2	32.33	35.18	28.35
Total (PC1 + PC2)	**84.02**	**84.45**	**79.38**

3.4 Infrared (IR) Spectral Characterization

In this study, defined wavenumber regions were selected for analysis: 3600 cm^{-1} – 2701 cm^{-1} (Region I), 1800 cm^{-1} – 1600 cm^{-1} (Region II), 1499 cm^{-1} – 1300 cm^{-1} (Region III), and 1201 cm^{-1} – 751 cm^{-1} (Region IV). Each region corresponds to characteristic functional group vibrations and structural features detected by ATR-FTIR analysis as listed in Table 3. The spectral peaks and patterns from each paper brand were examined in detail. Distinct differences in peak positions, intensities, and shapes were observed, which are attributed to variations in chemical composition between brands.

Region I (3600 cm^{-1} – 3000 cm^{-1}) corresponds to O–H stretching vibrations, which are associated with moisture content and hydrogen bonding in cellulose [25,33]. Most brands showed clear peaks in this range, with prominent peaks observed at 3335 cm^{-1} for Brands A and E, 3317 cm^{-1} for Brand D, and 3342 cm^{-1} for Brand G, indicating strong hydrogen bonding. In contrast, Brands C, F, J, K, L, and M exhibited broader, lower-intensity peaks, suggesting either lower moisture content or weaker hydrogen bonding interactions [45,46].

Region II (1800 cm^{-1} – 1600 cm^{-1}) is associated with C=O stretching vibrations of carbonyl groups present in cellulose derivatives or fillers, and H_2O bending vibrations around 1640 cm^{-1} [25,33,34]. This region reflects both water content and chemical additives in paper formulations. Across different brands, variations in this region were subtle but informative, showing shifts and peak intensity differences indicative of compositional variation in cellulose and filler materials.

Region III (1499 cm^{-1} – 1300 cm^{-1}) represents part of the fingerprint region, with peaks linked to calcium carbonate ($CaCO_3$) fillers, commonly used in paper

manufacturing [4,22,25,33,34]. Distinct peaks at 1420 cm^{-1} (Brand J), 1401 cm^{-1} (Brand F), and 1403 cm^{-1} (Brand M) indicated higher levels of $CaCO_3$ in these brands, suggesting differences in filler content that can aid in classification.

Region IV (1201 cm^{-1} – 751 cm^{-1}) also forms part of the fingerprint region, capturing characteristic vibrations of cellulose and carbonate compounds. Peaks around 1051–1056 cm^{-1} were common across brands, corresponding to C–O stretching in cellulose. Brands G and C showed slightly shifted peaks at 1058 cm^{-1}, reflecting minor compositional differences. Additionally, peaks at 872 cm^{-1} and 874 cm^{-1} in Brands F, J, and M are indicative of out-of-plane bending of carbonate ($CaCO_3$) and in-plane symmetric vibrations of C–O–C, supporting the presence of carbonate fillers and structural differences [46]. Figure 2 displays the IR spectra of each of the paper sample.

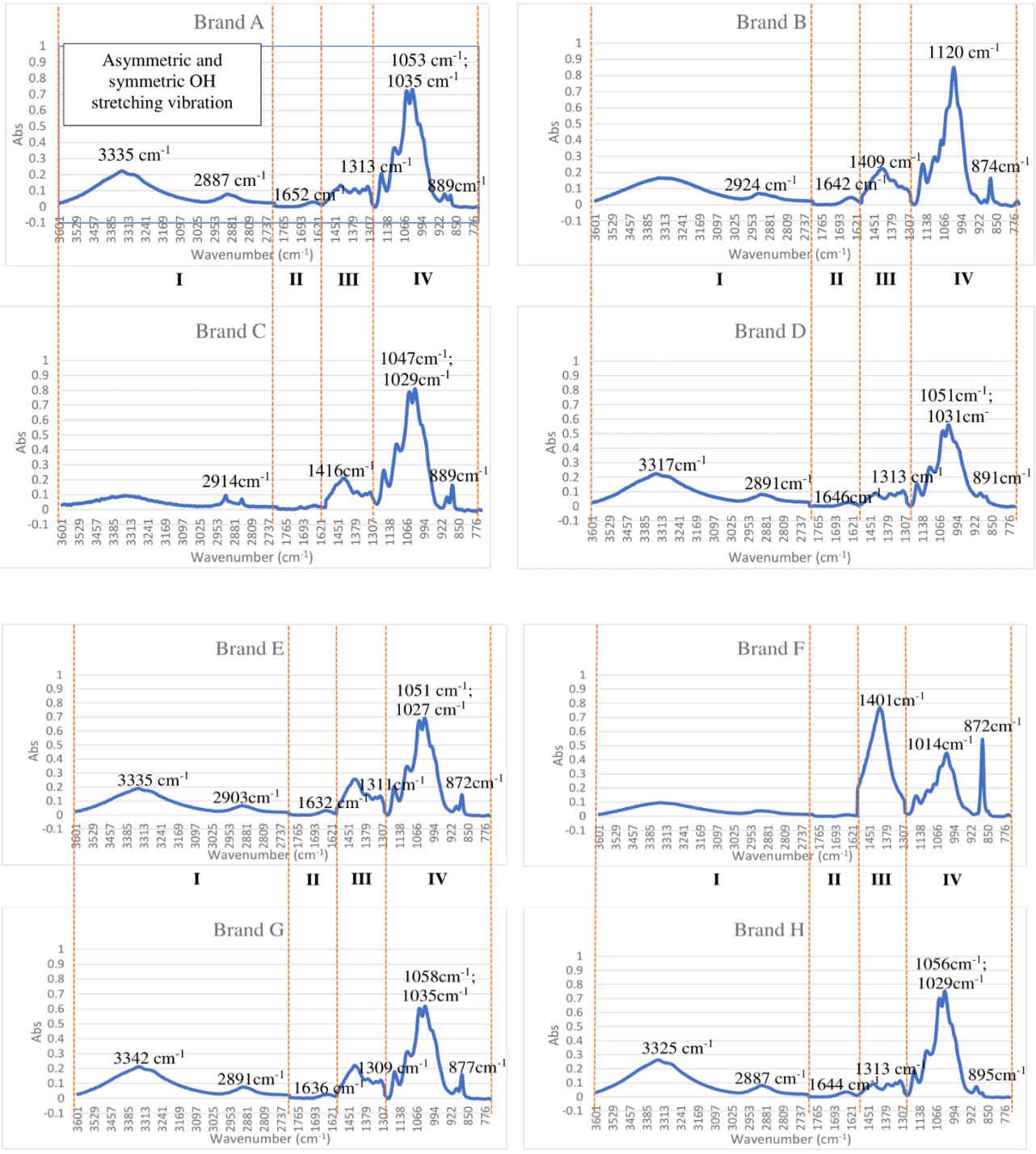

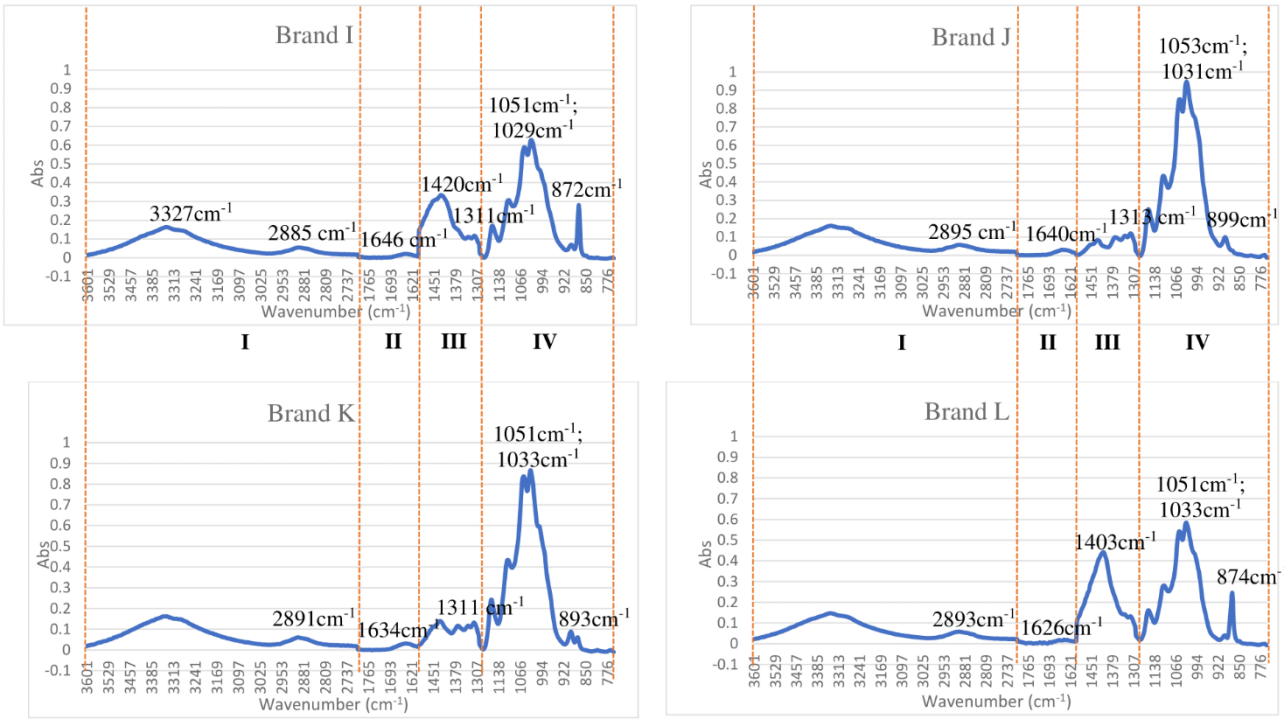

Figure 2 IR Spectra of Brand A to Brand G paper samples.

Table 3 Regions indicating corresponding wavenumbers and functional groups.

Region	Peak Type	Peaks Wavenumber (cm^{-1})	Peak assignments
I	Broad shoulder	3342, 3339, 3335, 3325, 3317	Asymmetric & symmetric OH stretching
3600-2701 cm^{-1}	Small to medium shoulder	2924, 2903, 2895, 2893, 2891, 2887, 2885,	CH stretching
II	Small peak	1652, 1646, 1644, 1643, 1640,	H_2O absorption
1800-1600 cm^{-1}		1634, 1632, 1626	
III	Small to medium peak	1457, 1432, 1420, 1418, 1416,	$CaCO_3$
1499-1300 cm^{-1}		1409, 1403	
		1362, 1366	CH^2 bending
	Small, medium, multiple	1313, 1311, 1309, 1300	Crystalized cellulose
IV	Strong sharp peak	1160, 1158, 1150, 1148	COC asymmetric stretching
1201-751 cm^{-1}			CC ring breathing
		1113, 1107, 1105, 1103, 1101, 1099, 1097	COC stretching
	Double peaks	1058, 1056,1053, 1051, 1047	CO stretching of secondary alcohol
		1035, 1033, 1031, 1029, 1027	Kaolin
	Small to moderate peaks	899, 895, 893, 891, 889, 874	CC; CCO; COC; OCO, COH
		877, 874, 872, 870	CO asymmetric stretch; $CaCO_3$, OCO bending

3.5 Principal Component Analysis (PCA)

Principal Component Analysis (PCA) was applied to explore and visualize the spectral differences among samples of the 12 paper brands. 3D score plot as shown in (Figure 3) shows how PCA reduces complex spectral data into principal components that capture the most significant variability. The first principal component (PC1) accounted for 66.26% of the total variance, followed by PC2 with 21% and PC3 with 12.7%, resulting in a cumulative variance of 99.96%. This indicates that nearly all the relevant information and variability between the paper brands were captured within these first three components.

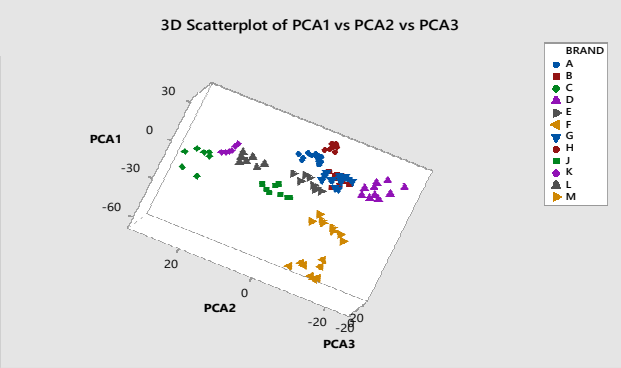

Figure 3 Three dimensional (3D) PCA score plot of the paper samples

The PCA results revealed clear clustering of the paper samples into 11 distinct groups, demonstrating strong brand-based separation. However, Brands B and G are convoluted, suggesting that while PCA is effective in revealing overall trends, it may not fully separate brands with highly similar compositions. This overlap likely results from similarities in manufacturing processes, raw materials, or the use of similar fillers and chemical treatments. Close examinations of the spectra of brands B and G as shown in Figure 4 reveal similar spectra features.

The similarities found in the spectra peaks and patterns in Brand B and G suggest that both brands contain similar or nearly identical base ingredients, chemical compositions, or key components, and physical properties in making the paper. However, even with similar spectra, small variations in peak positions or intensities can still reveal subtle differences in quality,

Although PCA is excellent for visualizing patterns and reducing data complexity, it is an unsupervised method that does not explicitly use class membership to maximize group separation. Therefore, for cases where clusters overlap or distinctions are subtle, it is necessary to apply Linear Discriminant Analysis (LDA). LDA is a supervised classification technique that takes predefined group labels into account and aims to maximize the variance between groups while minimizing the variance within groups. By following PCA with LDA, the classification accuracy can be significantly improved, enabling clearer discrimination between closely related brands concentration, or additional minor components unique to each brand.

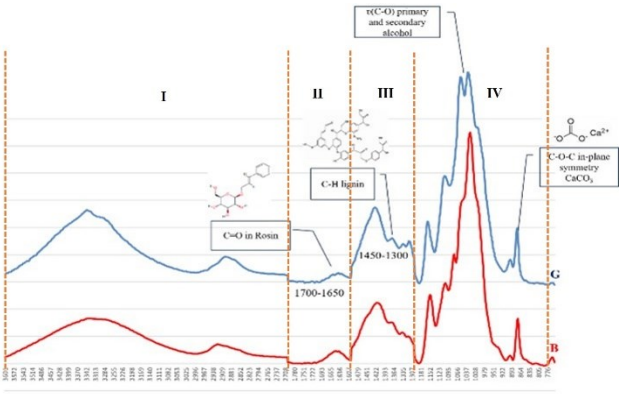

Figure 4 Similar characteristics in spectra peaks and patterns for Brand B and G.

3.6 Linear Discriminant Analysis (LDA)

LDA was applied as a supervised classification tool to maximize the separation between the 12 paper brands. Unlike PCA, which is an unsupervised method, LDA utilizes known group memberships to create functions that optimize discrimination between classes. The effectiveness of the LDA model is evaluated through Wilks' Lambda (λ), where values close to zero indicate a strong model fit [39]. As shown in Table 3, Wilks' Lambda values were consistently very low (λ = 0.018 for the first function), with significance levels of $p < 0.001$, demonstrating that the model is statistically significant and that there is a strong relationship between the independent (spectral data) and dependent (brand) variables.

Table 4 Wilks' Lambda of the Linear Discriminant Analysis.

Wilks' Lambda Table 4 Confusion matrix of the paper samples

Test of Function (s)	Wilk's Lambda	Chi-square	df	Sig.
1 through 3	.018	395.599	33	<.001
2 through 3	.113	215.024	20	<.001
3	.371	97.655	9	<.001

Table 5 Confusion matrix of the paper samples

		Classification Results [a, c] Predicted Group Membership												
	BRAND	**A**	**B**	**C**	**D**	**E**	**F**	**G**	**H**	**J**	**K**	**L**	**M**	**Total**
Original Count	**A**	6	4	0	2	0	0	0	0	1	0	0	0	**13**
	B	0	9	0	0	0	0	0	0	0	0	0	0	**9**
	C	1	0	6	0	0	0	0	0	0	0	0	0	**7**
	D	0	0	1	8	0	0	0	0	0	1	0	0	**10**
	E	0	0	0	0	6	1	1	0	0	0	0	0	**8**
	F	0	0	0	0	0	8	0	0	0	0	0	0	**8**
	G	0	0	0	0	2	0	10	0	0	1	0	0	**13**
	H	0	0	0	0	0	0	0	9	0	0	0	0	**9**
	J	0	0	0	0	0	0	0	1	7	0	0	0	**8**
	K	0	0	0	0	0	0	0	0	0	5	1	0	**6**
	L	0	0	0	0	0	0	0	0	0	2	5	1	**8**
	M	0	0	0	0	0	0	0	0	0	1	0	7	**8**
Cross-validated Count	**A**	6	4	0	2	0	0	0	0	1	0	0	0	**13**
	B	0	9	0	0	0	0	0	0	0	0	0	0	**9**
	C	1	0	6	0	0	0	0	0	0	0	0	0	**7**
	D	0	1	8	0	0	0	0	0	0	1	0	0	**10**
	E	0	0	0	0	6	1	1	0	0	0	0	0	**8**
	F	0	0	0	0	0	8	0	0	0	0	0	0	**8**
	G	0	0	0	0	2	0	8	2	0	1	0	0	**13**
	H	0	0	0	0	1	0	0	8	0	0	0	0	**9**
	J	0	0	0	0	0	0	0	1	7	0	0	0	**8**
	K	0	0	0	0	0	0	0	0	0	3	3	0	**6**
	L	0	0	0	0	0	0	0	0	0	3	4	1	**8**
	M	0	0	0	0	0	0	0	0	0	1	0	7	**8**

a. 80.4% of original grouped cases correctly classified.
b. Cross validation is done only for those cases in the analysis. In cross validation, each case is classified by the functions derived from all cases other than case.
c. 74.8% of cross-validated grouped cases correctly classified.

The classification results in Table 5 show that 80.4% of the original grouped cases were correctly classified, while cross-validation yielded a classification accuracy of 74.8% [47]. The slight reduction in accuracy after cross-validation is expected, as this process evaluates the model's robustness and ability to classify new, unseen data. The close clustering of Brands B and G, as previously observed in PCA, influenced this overlap and reduced classification performance between those brands.

The classification results also further highlight the model's predictive power. Most brands were classified correctly, with only minor misclassifications, primarily between brands with similar spectral characteristics. For example, Brand G showed some misclassification into Brand E and vice versa, likely due to compositional similarities.

Table 6 provides a more detailed look at classification performance using accuracy, precision (specificity), recall (sensitivity), and F1 scores. The overall accuracy (TP + TN) of 82.05% demonstrates the model's reliability. Brand F and Brand H, in particular, performed exceptionally well, each achieving 99% accuracy, 100% sensitivity, and high F1 scores of 94%, reflecting both excellent precision and recall. In contrast, Brand A exhibited more modest performance, with 94% accuracy and a lower F1 score of 58%, indicating challenges in balancing precision and recall for this brand. Misclassifications in Brand A likely stem from spectral overlap with other brands, especially those with similar fiber or filler compositions.

Table 6 Classification performance

BRAND	A	B	C	D	E	F	G	H	J	K	L	M
Accuracy	94%	97%	77%	97%	97%	99%	98%	99%	98%	98%	95%	98%
Specificity/ Performance	76%	76%	90%	84%	83%	89%	86%	100%	92%	87%	79%	88%
Sensitivity/ Recall	46%	100%	86%	80%	75%	100%	83%	89%	88%	83%	63%	88%
F1 Score	58%	87%	88%	82%	79%	94%	85%	94%	90%	85%	70%	88%
Overall Accuracy		**TP+TN**			**82.05%**							

4.0 CONCLUSION

The significance of this work lies in its ability to provide a rapid, non-destructive, and objective method for discriminating paper samples of different brands from different manufacturers, which can be highly valuable in forensic document examination. This approach can aid in source attribution, verification of document authenticity, and detection of forgeries, supporting legal investigations and court proceedings with scientific evidence. For future work, it is recommended to expand the study by incorporating a larger number of paper brands, different paper types, and varying paper weights to further validate the model's applicability across diverse samples. Additionally, integrating other analytical techniques such as Raman spectroscopy or hyperspectral imaging, along with advanced machine learning algorithms, could improve classification accuracy, particularly for brands with closely overlapping characteristics. Establishing a comprehensive spectral database for paper analysis could also enhance forensic reference capabilities and support broader application in criminal, civil, and regulatory cases involving questioned documents.

Acknowledgements

The authors acknowledge the support given by the staff of the Advanced Analytical Laboratory (MAL), School of Health Sciences, USM Kubang Kerian and the international industry grant (R504-LR-GAL008-0006150281-H124) awarded by HFDE Services Pte. Ltd. (Singapore) which has enabled this study to be conducted.

Conflicts of Interest

The authors declare that there is no conflict of interest regarding the publication of this paper.

References

[1] Levinson, J. 2001. *Questioned Documents: A Lawyer's Handbook*. Great Britain: Academic Press.
[2] McGaw, E. A., D. W. Szymanski, and R. W. J. Smith. 2009. Determination of Trace Elemental Concentrations in Document Papers for Forensic Comparison Using Inductively Coupled Plasma–Mass Spectrometry. *Journal of Forensic Sciences*. 54(5): 1163–1170.
[3] Kumar, R., V. Kumar, and V. Sharma. 2017. Fourier Transform Infrared Spectroscopy and Chemometrics for the Characterization and Discrimination of Writing/Photocopier Paper Types: Application in Forensic Document Examinations. *Spectrochimica Acta Part A: Molecular and Biomolecular Spectroscopy*. 170: 19–28.
[4] Causin, V., C. Marega, C. Marigo, R. Casamassima, G. Peluso, and L. Ripani. 2010. Forensic Differentiation of Paper by X-Ray Diffraction and Infrared Spectroscopy. *Forensic Science International*. 197(1–3): 70–74.
[5] Fardim, P., and B. Holmbom. 2005. ToF-SIMS Imaging: A Valuable Chemical Microscopy Technique for Paper and Paper Coatings. *Applied Surface Science*. 249 (1–4): 393–407.
[6] Van Es, A., J. De Koeijer, and G. Van der Peijl. 2009. Discrimination of Document Paper by XRF, LA–ICP–MS and IRMS Using Multivariate Statistical Techniques. *Science & Justice*. 49(2): 120–126.
[7] Sarkar, A., S. K. Aggarwal, and D. Alamelu. 2010. "Laser Induced Breakdown Spectroscopy for Rapid Identification of Different Types of Paper for Forensic Application." *Analytical Methods* 2 (1): 32–36.
[8] Manso, M., and M. Carvalho. 2007. "Elemental Identification of Document Paper by X-Ray Fluorescence Spectrometry. *Journal of Analytical Atomic Spectrometry*. 22(2): 164–170.
[9] Manso, M., S. Pessanha, and M. Carvalho. 2006. Artificial Aging Processes in Modern Papers: X-Ray Spectrometry Studies. *Spectrochimica Acta Part B: Atomic Spectroscopy*. 61(8): 922–928.
[10] Rožić, M., R. M. Mačefat, and V. Oreščanin. 2005. Elemental Analysis of Ashes of Office Papers by EDXRF Spectrometry. *Nuclear Instruments and Methods in Physics Research Section B*. 229(1): 117–122.
[11] Skipperud, L., B. Salbu, and E. Hagebø. 1998. Transfer, Pathways, Enrichment and Discharge of Trace Elements in the Pulp Industry Measured by Means of Neutron Activation Analysis. *Science of the Total Environment*. 216(1–2): 133–146.
[12] Trejos, T., A. Flores, and J. R. Almirall. 2010. Micro-Spectrochemical Analysis of Document Paper and Gel Inks by Laser Ablation Inductively Coupled Plasma Mass Spectrometry and Laser Induced Breakdown Spectroscopy. *Spectrochimica Acta Part B: Atomic Spectroscopy*. 65(11): 884–895.
[13] Jones, K., S. Benson, and C. Roux. 2016. The Forensic Analysis of Office Paper Using Oxygen Isotope Ratio Mass Spectrometry. Part 1: Understanding the Background Population and Homogeneity of Paper for the Comparison and Discrimination of Samples. *Forensic Science International*. 262: 97–107.
[14] Jones, K., S. Benson, and C. Roux. 2016. The Forensic Analysis of Office Paper Using Oxygen Isotope Ratio Mass Spectrometry. Part 2: Characterizing the Source Materials and the Effect of Production and Usage on the δ18O Values of Cellulose and Paper. *Forensic Science International*. 268: 151–158.

[15] Jones, K., S. Benson, and C. Roux. 2013. "The Forensic Analysis of Office Paper Using Carbon Isotope Ratio Mass Spectrometry. Part 3: Characterizing the Source Materials and the Effect of Production and Usage on the δ13C Values of Paper." *Forensic Science International* 1–3: 355–364.
[16] Lukens, H. R., H. L. Schlesinger, D. M. Settle, and V. P. Guinn. 1970. Forensic Neutron Activation Analysis of Paper. San Diego, CA: Gulf General Atomic.
[17] Spence, L. D., R. B. Francis, and U. Tinggi. 2002. Comparison of the Elemental Composition of Office Document Paper: Evidence in a Homicide Case. *Journal of Analytical Atomic Spectrometry*. 47(3): 648–651.
[18] Lennard, C., M. M. El-Deftar, and J. Robertson. 2015. Forensic Application of Laser-Induced Breakdown Spectroscopy for the Discrimination of Questioned Documents. *Forensic Science International*. 254: 68–79.
[19] Yayli, M., O. K. Koksal, G. Apaydin, M. Sirin, E. Cengiz, and H. Baltas. 2017. Comparison of Elemental Analysis for Different Kinds of Papers by Using Energy Dispersive X-Ray Spectrometer. *Asian Journal of Chemistry*. 29(6): 1301–1307.
[20] Zięba-Palus, J., A. Wesełucha-Birczynska, B. Trzcinska, R. Kowalski, and P. Moskal. 2017. Analysis of Degraded Papers by Infrared and Raman Spectroscopy for Forensic Purposes. *Journal of Molecular Structure*. 1140: 154–162.
[21] Chiriu, D., P. C. Ricci, G. Cappellini, and C. M. Carbonaro. 2018. Ancient and Modern Paper: Study on Ageing and Degradation Process by Means of Portable NIR μ-Raman Spectroscopy. *Microchemical Journal*. 138: 26–34.
[22] Udriştioiu, F. M., I. Gh. Tănase, A. A. Bunaciu, and H. Y. Aboul-Enein. 2012. Paper Analysis: Nondestructive and Destructive Analytical Methods. *Applied Spectroscopy Reviews*. 47 (7): 550–570.
[23] Zięba-Palus, J., B. Trzcinska, A. Wesełucha-Birczynska, P. Moskal, and J. Sacharz. 2020. The Sequence of Changes Observed during Degradation Process of Paper by the Use of UV/VIS and FTIR Spectrometry with Application of PCA and 2D Correlation Method for Forensic Purposes. *Journal of Molecular Structure*. 1205: 127651.
[24] Causin, V., R. Casamassima, G. Marruncheddu, G. Peluso, and L. Ripani. 2012. The Discrimination Potential of Diffuse-Reflectance Ultraviolet–Visible–Near Infrared Spectrophotometry for the Forensic Analysis of Paper. *Forensic Science International*. 216(1–3): 163–167.
[25] Pavithra, R., S. Gunasekaran, E. Sailatha, and S. Kamatchi. 2015. Investigations on Paper Making Raw Materials and Determination of Paper Quality by FTIR-UATR and UV-Vis DRS Spectroscopy. *International Journal of Current Research and Academic Review*. 3: 42–59.
[26] Bajpai, P., and R. Kondo. 2012. *Biotechnology for Pulp and Paper Processing*. Springer.
[27] Tiňo, R., K. Vizárová, J. Provazníková, S. Šutý, and S. Kirschnerová. 2018. Utilization of Statistical Analysis of FT-IR Spectra in Forensic Examination of Paper. *Chemical Papers*. 72(9): 2265–2272.
[28] Trafela, T., M. Strlič, J. Kolar, D. A. Lichtblau, M. Anders, D. Pucko Mencigar, and B. Pihlar. 2007. Nondestructive Analysis and Dating of Historical Paper Based on IR Spectroscopy and Chemometric Data Evaluation. *Analytical Chemistry*. 79(16): 6319–6323.
[29] Silva, C. S., M. F. Pimentel, J. M. Amigo, C. García-Ruiz, and F. Ortega-Ojeda. 2018. Chemometric Approaches for Document Dating: Handling Paper Variability. *Analytica Chimica Acta*. 1031: 28–37.
[30] Xia, J., J. Zhang, Y. Zhao, Y. Huang, Y. Xiong, and S. Min. 2019. Fourier Transform Infrared Spectroscopy and Chemometrics for the Discrimination of Paper Relic Types. *Spectrochimica Acta Part A: Molecular and Biomolecular Spectroscopy*. 219: 8–14.
[31] Xia, J., Y. Huang, J. Zhang, X. Du, H. Yan, Q. Li, Y. Li, Y. Xiong, and S. Min. 2020. Development of a Chemometric Methodology Based on FTIR Spectra for Paper Dating. *Cellulose*. 27: 5323–5335.
[32] Enders, A. A., N. North, C. Fensore, J. Vélez Alvarez, and H. Allen. 2021. Functional Group Identification for FTIR Spectra Using Image-Based Machine Learning Models. *Analytical Chemistry*. 93(28): 9711–9718.
[33] Sharma, V., J. Kaur, and R. Kumar. 2020. Proof of Concept Study for Paper Discrimination and Age Estimation through Its Degradation Process by ATR-FTIR Spectroscopy and Chemometric Models. *Australian Journal of Forensic Sciences*. 1–24.
[34] Farid, S., M. A. Kasem, A. F. Zedan, G. G. Mohamed, and A. El-Hussein. 2021. Exploring ATR Fourier Transform IR Spectroscopy with Chemometric Analysis and Laser Scanning Microscopy in the Investigation of Forensic Documents Fraud. *Optics & Laser Technology*. 135: 106704.
[35] Vahur, S., L. Eero, J. Lehtaru, K. Virro, and I. Leito. 2019. Quantitative Non-Destructive Analysis of Paper Fillers Using ATR-FT-IR Spectroscopy with PLS Method. *Analytical and Bioanalytical Chemistry*. 411: 5127–5138.
[36] Nandiyanto, A. B. D., R. Oktiani, and R. Ragadhita. 2019. How to Read and Interpret FTIR Spectroscope of Organic Material. *Indonesian Journal of Science and Technology*. 4(1): 97–118.
[37] Sauzier, G., W. van Bronswijk, and S. W. Lewis. 2021. Chemometrics in Forensic Science: Approaches and Applications. *Analyst*. 146(8): 2415–2448.
[38] Mendlein, A. N. 2011. Instrumental and Chemometric Analysis of Automotive Clear Coat Paints by Micro Laser Raman and UV Microspectrophotometry. PhD diss. Purdue University.
[39] Kumar, R., and V. Sharma. 2018. Chemometrics in Forensic Science. *Trends in Analytical Chemistry*. 105: 191–201.
[40] Kher, A., M. Mulholland, B. Reedy, and P. Maynard. 2001. Classification of Document Papers by Infrared Spectroscopy and Multivariate Statistical Techniques. *Applied Spectroscopy*. 55 (9): 1192–1198.
[41] Kumar, R., V. Kumar, and V. Sharma. 2015. Discrimination of Various Paper Types Using Diffuse Reflectance Ultraviolet–Visible Near-Infrared (UV-Vis-NIR) Spectroscopy: Forensic Application to Questioned Documents. *Applied Spectroscopy*. 69(6): 714–720.
[42] Buzzini, P., J. Curran, and C. Polston. 2021. Comparison between Visual Assessments and Different Variants of Linear Discriminant Analysis to the Classification of Raman Patterns of Inkjet Printer Inks. *Forensic Chemistry*. 24: 100336.
[43] Nur Atiqah, Z., D. Ismail, W. N. S. M. Desa, and N. F. N. Hassan. 2023. Evaluating the Potential of Chemometrics Techniques as Rapid Screening Tools for Black Gel Inks Discrimination. *Malaysian Journal of Analytical Sciences*. 27(6): 1205–1215.
[44] Rinnan, Å., F. van den Berg, and S. B. Engelsen. 2009. Review of the Most Common Pre-Processing Techniques for Near-Infrared Spectra. *Trends in Analytical Chemistry*. 28(10): 1201–1222.
[45] Łojewski, T., P. Miśkowiec, M. Molenda, A. Lubańska, and J. Łojewska. 2010. Artificial versus Natural Ageing of Paper: Water Role in Degradation Mechanisms. *Applied Physics A*. 100: 625–633.
[46] Hajji, L., A. Boukir, J. Assouik, S. Pessanha, J. L. Figueirinhas, and L. Carvalho. 2016. Artificial Aging Paper to Assess Long-Term Effects of Conservative Treatment: Monitoring by Infrared Spectroscopy (ATR-FTIR), X-Ray Diffraction (XRD), and Energy Dispersive X-Ray Fluorescence (EDXRF). *Microchemical Journal*. 124: 646–656.
[47] Everitt, B. S., and G. Dunn. 2001. *Applied Multivariate Data Analysis*. 2nd ed. London: Arnold.

Supplementary Files

Repeatability and Reproducibility Studies

The data collected were tested for repeatability and reproducibility studies. Table S1 depicts the relative standard deviation (RSD%) results from the repeatability studies. The RSD% reflects a range between 3.14% to 4.34% which reflects an acceptable level of repeatability (<5%).

The reproducibility studies shown in Table S2 and S3 for intra and inter-sheet variations respectively, indicates the RSD variations between and among the paper is less than 6%. This explain the spread of composition in the paper around the mean is small, meaning the measurements are consistent and reliable. This level of consistency in the data shows that the variability between the samples are at an acceptable level for further analysis.

Table S1: Repeatability studies

	3347 cm^{-1}	**2892 cm^{-1}**	**1644 cm^{-1}**	**1316 cm^{-1}**	**1028 cm^{-1}**	**1100 cm^{-1}**
1	0.23643	0.07911	0.02984	0.11560	0.73192	0.31937
2	0.22039	0.07941	0.02907	0.11101	0.71882	0.31950
3	0.23378	0.08449	0.03009	0.11634	0.68149	0.32652
4	0.22166	0.08053	0.03040	0.12020	0.72348	0.34724
5	0.21485	0.08099	0.02828	0.10931	0.69254	0.33510
6	0.21755	0.07437	0.02679	0.11434	0.74134	0.32846
7	0.23356	0.07932	0.03066	0.12399	0.74695	0.35542
Avg.	0.22546	0.07975	0.02930	0.11583	0.71951	0.33309
std	0.00819	0.002784	0.00127	0.00468	0.02259	0.01276
%RSD	**3.64%**	**3.49%**	**4.34%**	**4.05%**	**3.14%**	**3.83%**

Table S2: Reproducibility (Intra-sheet)

	3347 cm^{-1}	**2892 cm^{-1}**	**1644 cm^{-1}**	**1316 cm^{-1}**	**1028 cm^{-1}**	**1100 cm^{-1}**
1	0.23436	0.07401	0.02947	0.11908	0.75619	0.34436
2	0.22346	0.08000	0.02937	0.11101	0.70146	0.31950
3	0.22399	0.08134	0.03099	0.12020	0.70786	0.34724
4	0.22882	0.07399	0.02725	0.11426	0.71922	0.31774
5	0.22078	0.07356	0.03157	0.11525	0.71284	0.32650
6	0.23325	0.07619	0.02999	0.12365	0.77365	0.35567
7	0.20882	0.07770	0.02901	0.11445	0.72542	0.33678
Avg.	0.22292	0.07668	0.02966	0.11684	0.72809	0.33540
std	0.00928	0.00288	0.00130	0.00399	0.02479	0.01350
%RSD	**4.16%**	**3.76%**	**4.39%**	**3.42%**	**3.41%**	**4.03%**

Table S3: Reproducibility (Inter-sheet)

	3347 cm^{-1}	2892 cm^{-1}	1644 cm^{-1}	1316 cm^{-1}	1028 cm^{-1}	1100 cm^{-1}
1	0.25756	0.07923	0.03442	0.11399	0.74653	0.31880
2	0.25442	0.08088	0.03480	0.10548	0.68439	0.29605
3	0.23350	0.07645	0.03394	0.12262	0.74308	0.34966
4	0.24234	0.07761	0.03444	0.11585	0.73634	0.34203
5	0.23423	0.07865	0.03239	0.11018	0.72394	0.32279
6	0.23153	0.07329	0.02974	0.11908	0.77666	0.34436
7	0.22166	0.08053	0.03040	0.12020	0.72348	0.34724
Avg.	0.23932	0.07809	0.03288	0.11534	0.73349	0.33156
std	0.01196	0.00242	0.00192	0.00556	0.02601	0.01831
%RSD	**5.00%**	**3.11%**	**5.84%**	**4.82%**	**3.55%**	**5.52%**

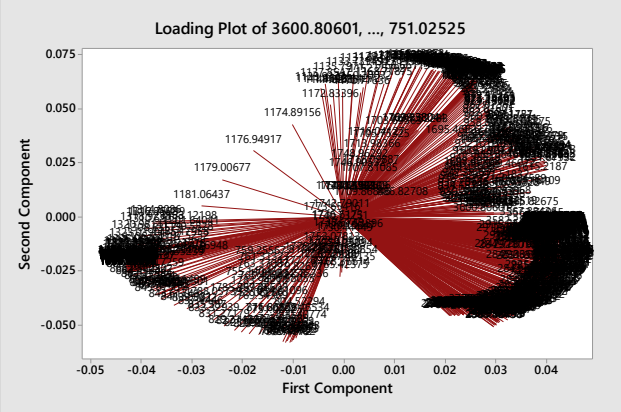

Figure S1: Loading Plot

Figure S1 shows the loading plot for the dataset. The dense clustering near the origin (center) suggests that many wavenumbers have minimal contribution to the first two components, which explain the importance of variable selection or dimensionality reduction prior to classification